NM IMAGES FILTERING USING NPR QMF FILTERS DEPENDENT ON THE IMAGES SPECTRUM

Cvetko D. Mitrovski and Mitko B. Kostov

Abstract – **In this paper we present our approach on pre-processing of the heart region dynamic NM images. The presented method combines a Discrete Wavelet Transform (DWT) realized via linear phase near perfect reconstruction (NPR) quadrature mirror filters (QMF) with a specific strategy for selecting the filters cut-off frequency and the filtering into the time direction of the consecutive images. The aim of the method is to develop sophisticated diagnostic software that would automatically offer the optimal positions and the shapes of the regions of interest needed for heart studies.**

Keywords – **NM images, QMF, wavelet-domain filtering.**

I. INTRODUCTION

Nuclear Medicine (NM) images are diagnostic digital images, which provide both anatomical and functional data for the patients. Due to the nature of the gamma ray emission process and due to the operational characteristics of the gamma cameras (low count levels, scatter, attenuation, and electronic noises in the detector/camera), they have a low signal-to-noise ratio (SNR) [1]. Therefore, a suitable image pre-processing must precede the NM images analysis in order to provide an accurate recognition of patient's anatomical data.

This paper presents our proposal on pre-processing of NM heart-region images. The images are processed in the discrete wavelet transform domain with linear phase NPR QMF filters. The filters are designed to have a cut-off frequency dependent on the images frequency spectrum. In addition, while filtering a particular image, information from its adjacent images is used.

The paper is organized as follows. Section II models the NM images creation process and formulates the problems due which raw NM images should be pre-processed. The wavelet theory and wavelet-domain filtering are briefly outlined in Section III. Section IV introduces our proposal for a suitable filtration of heart-region NM images. Examples for illustration and comparison are given in Section V, while the conclusion is given in Section VI.

II. NM IMAGES CREATION PROCESS

The process of generating the NM images starts after injection of certain, small dose (for safety reasons) of suitably chosen radioactive material, into the body of a patient. The radionuclide spreads and mixes with the blood on its way to the heart through the vena cava superior which results with some very complicated and fast changing radionuclide concentration distribution function $\rho(x, y, z, t)$ [2]. This process could be recorded as a set of a finite number of NM images by accumulating emitted gamma rays in NxN matrices, for a certain period τ. Each image contains rather high level of noise caused by: a) mixing the radionuclide with the blood and the spreading of this mixture, b) hydrodynamic processes in the blood vessels caused by the pumping work of the heart and c) by the randomness of the gamma rays emission and their detection by the gamma camera. Considering this, the raw images (Fig. 1) should be adequately pre-processed in order to extract the anatomy information about the position of the vena and the heart.

Cvetko D. Mitrovski and Mitko B. Kostov are with the Faculty of Technical Sciences, I.L.Ribar bb, 7000 Bitola, Macedonia, E-mail: {cvetko.mitrovski, mitko.kostov}@uklo.edu.mk

III. AN OVERVIEW OF THE DISCRETE WAVELET TRANSFORM

The Discrete Wavelet Transform (DWT) decomposes a signal into a set of orthogonal components describing the signal variation across the scale [3]. The orthogonal components are generated by dilations and translations of a prototype function ψ called mother wavelet.

In analogy with other function expansions, a function *f* may be written for each discrete coordinate *t* as a sum of a wavelet expansion up to certain scale *J* plus a residual term, that is:

$$f(t) = \sum_{j=1}^{J} \sum_{k=1}^{2^{-j}M} d_{jk} \psi_{jk}(t) + \sum_{k=1}^{2^{-J}M} c_{Jk} \phi_{Jk}(t) \qquad (2)$$

where ψ_{jk} is component obtained by dilation and translation of the mother wavelet. The approximation coefficients c_{Jk} contain the signal identity while the detail coefficients d_{jk} likely contain noise and need to be processed in order to remove the noise.

The most popular form of wavelet-based filtering, commonly known as *Wavelet Shrinkage* [4], [5], involves filtering the contribution of a particular wavelet basis function in the signal expansion by weighting the corresponding wavelet coefficient by a number $0 \le h_i \le 1$:

$$\hat{w}_i = w_i \cdot h_i \qquad (3)$$

In the wavelet shrinkage, the filter corresponds to either the "hard threshold" nonlinearity

$$h_i^{(\text{hard})} = \begin{cases} 1, & \text{if } |w_i| \ge \tau \\ 0, & \text{if } |w_i| < \tau \end{cases} \qquad (4)$$

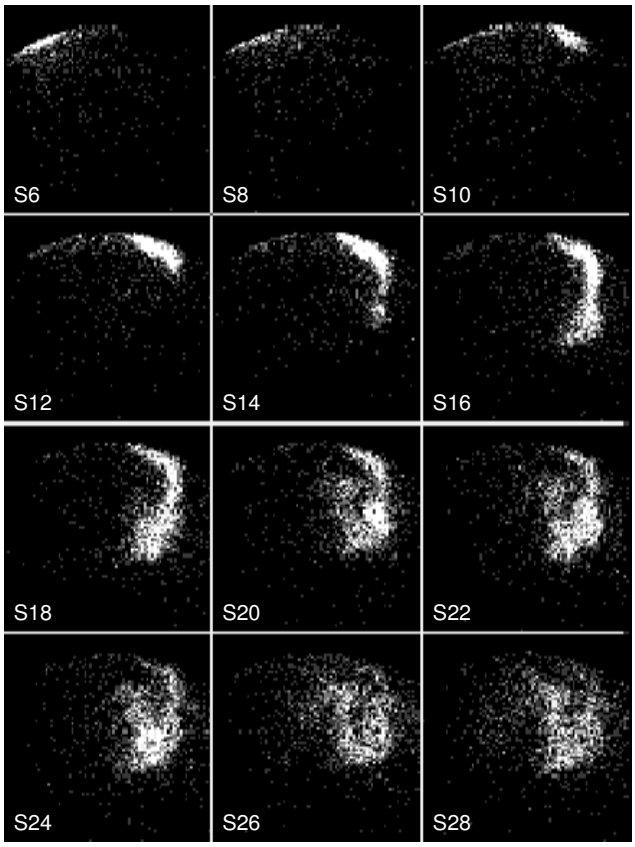

Fig. 1. Sequence of enhanced noised images (τ=0.4 s)

or the "soft threshold" nonlinearity

$$h_i^{(\text{soft})} = \begin{cases} 1 - \dfrac{\tau \,\text{sgn}(w_i)}{w_i}, & \text{if } |w_i| \geq \tau \\ 0, & \text{if } |w_i| < \tau \end{cases} \qquad (5)$$

with a user-specified threshold level τ.

IV. Filtration of NM Images

The chest region NM images recorded immediately after the injection of the radionuclide into the patient show the spreading of rather compact mass of radionuclide through the vena (Fig. 1). In spite of that, these images contain high level of spatially distributed noise in a form of isolated pixels in the neighbourhood of the vena. After a dozen of experiments [6], we concluded that the best method for removing this noise is to use the autocorrelation low-pass 2D filtering technique on the each raw NM image, S_l , l=1,2,…,k. and obtain a new set of initially filtered images $S_l^{(1)}$; l=1,2,..,k.

Since the dynamic images are consecutive, it can be expected that each image contains certain information that can be used for further pre-processing of its time neighbouring images [7]. In order to use this information we create *NxN, k*-length vectors by joining the pixel intensities at the position (*i,j*) of the initially filtered images (Fig.2). These vectors

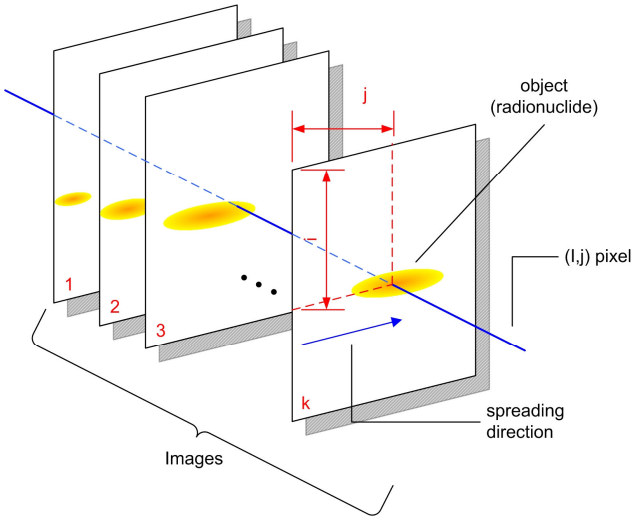

Fig. 2. Creating vectors by joining the pixels that are located at same position

contain some isolated peaks which are result of the noise, still present in the images $S_l^{(1)}$; l=1,2,..,k. In order to eliminate these peaks we apply low-pass wavelet filtering to all of these vectors and the obtained results are used to construct the new set of filtered images $S_l^{(2)}$; l=1,2,..,k.

The further processing of those images is based on their 2D power spectrum characteristics. Actually, for each image $S_l^{(2)}$, l=1,2,…,k, we determine its power 2D spectrum and we determine its cut-off frequency. The power spectrum of all the chest region NM images, especially in their initial phase (while the radionuclide is spreading trough the vena), is concentrated on low frequencies in an ellipse like region, as illustrated in Fig.3. The larger axes of those regions are orthogonal on the direction of the radionuclide spreading which is used for determining the cut of frequency of each image $S_l^{(2)}$, l=1,2,…,k, [8].

In addition, the heart region images contain quantum noise that obeys Poisson law [9]. It means that the level of the noise is higher on the parts of the images where the image signal is higher and vice versa. Therefore for further denoising of the images we propose processing in a DWT transform domain. By using the DWT we divide the image signal on two components: a) an approximation part and b) a part with details. After that we apply wavelet shrinkage method (5) only on the wavelet coefficients of the part with details (consist noise concentrated in the high frequency components) and return back into the image domain, $S_l^{(3)}$, l=1,2,…,k, by applying IDWT on the modified wavelet coefficients.

By applying the wavelet shrinkage we discard the wavelet coefficients with low SNR. Therefore the signal perfect reconstruction (PR) is not possible. Hence we decompose the images by using a NPR QMF bank instead of using standard wavelet filters. With this we provide better frequency response and increase the design flexibility since the filter cut-off frequency, filter length and overall reconstruction error of the designed QMF bank are design parameters which has to be adjusted to each image $S_l^{(2)}$, l=1,2,…,k.

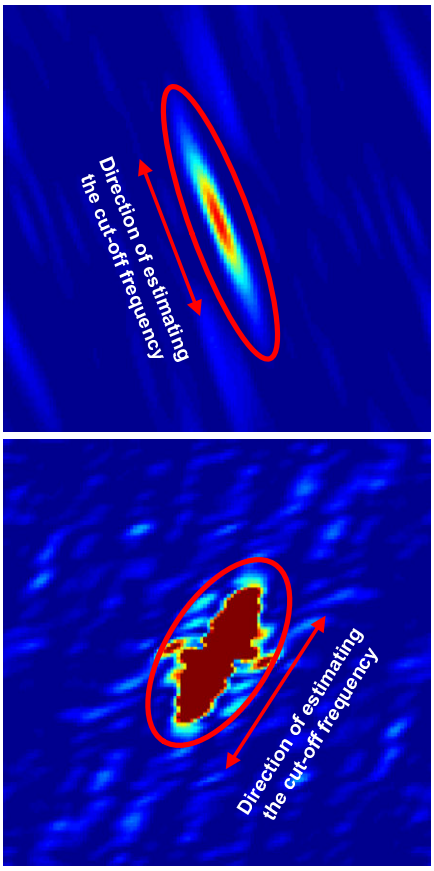

Fig. 3. 2D power spectrum of real NM images after applied autocorrelation and 1D wavelet filtering (normalized)
a) image with index 7, b) image with index 14

At last we form the resultant image from the filtrated images according to the formula:

$$S_R(i,j) = \max\{ S_1^{(3)}(i,j), S_2^{(3)}(i,j), \ldots, S_k^{(3)}(i,j) \},$$
$$1 \le i, j \le N \quad (6)$$

which consists the contours of the vena and the heart, Fig 4a.

A step-by-step description of the proposed algorithm for extracting the relevant anatomical data from a series of raw NM images is as follows:

1. Apply the autocorrelation technique to each image separately;
2. Apply the wavelet filtering to vectors created from all the images obtained in step 1 by joining the pixels that are located at same position and reconstruct the images;
3. Estimate filter cut-off frequency for each image obtained in step2 according their 2D spectrum;
4. Apply the standard soft-thresholding level 1 to each processed image from step 2 by using NPR QMF filter bank with adjusted cut of frequency determined in step3;

TABLE 1
IMAGES ENERGY CONCENTRATION AND CUT-OFF FREQUENCIES OF THE NPR QMF ANALYSYS LOWPASS FILTERS

Image No	Highest boundary frequency of the images power spectrum (*π)	Filter cut-off frequency (*π)
5-7	0.4574; 0.5969; 0.5659	0.7
8-10	0.4109; 0.3333; 0.2403	0.7; 0.5; 0.5
11-12	0.2558; 0.2248	0.5
13-14	0.2093	0.5
15-16	0.1318; 0.0853	0.5; 0.3
17-18	0.0698; 0.0543	0.3
19-22	0.0388	0.3
23	0.0543	0.3
24-30	0.0388	0.3

TABLE 2
PROTOTYPE FILTER COEFFICIENTS OF THE USED QMF BANKS

Filter coefficients	Filter cut-off frequency 0.3 (*π)	Filter cut-off frequency 0.5 (*π)	Filter cut-off frequency 0.7 (*π)
h(1) = h (12)	-0.0349	0.0276	0.0123
h(2) = h (11)	-0.1485	0.0841	0.0313
h(3) = h (10)	-0.0632	-0.0927	-0.0473
h(4) = h (9)	0.1146	-0.1600	-0.1129
h(5) = h (8)	0.3381	0.1933	0.1764
h(6) = h (7)	0.5010	0.6547	0.6473

5. Form the resultant image from the filtrated images.

V. EXPERIMENTAL RESULTS

In this Section, we illustrate the effects of applying our approach and compare these effects with the results obtained by using the conventional approach. Both approaches are applied on a same set of 24 sequential dynamic NM images (Fig. 1), recorded with resolution 128x128 and accumulation time $\tau = 0.4$ [s].

In the experiments, first we process the images by applying the autocorrelation technique which suppresses the salt and pepper noise. Next, we apply 1D wavelet filtering to vectors created by joining the pixels located at same positions in the images. In view of used filters, we decompose the vectors by using db3 wavelet and reconstruct them by using the same wavelet, but only from the approximation coefficients at level 1. After processing there are no abrupt changes and isolated peaks in the processed vectors.

Further, we design suitable NPR QMF banks needed for computing 2D DWT of each image (obtained in step 2) by using the algorithm described in [10]. For this reason, we divide the set of images in three groups according to the images energy concentration and for each of them we design a NPR QMF filter bank with a proper cut-off frequency. The frequencies where the images energy is concentrated and the proposed filters cut-off frequencies are given in Table 1, while

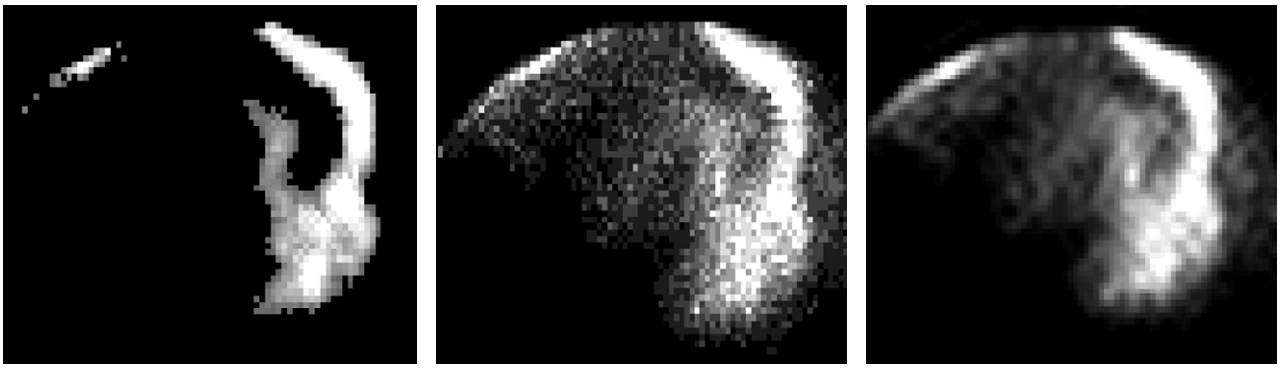

Fig. 4. The vena and the heart a) proposed approach b) conventional approach c) low-pass filtering of the image in b)

the prototype filters coefficients are given in Table 2. For particular image the frequencies where the image energy is concentrated are estimated after discarding pixels with intensity lower than 33% of the maximal image intensity. The designed filters have linear phase (zero at π), good pass-band, least squares stop-band and narrow transition band. In order to reduce the ringing effect the filters length was set to 12. The overall reconstruction error of the designed QMF bank is set to 0.001. Further, by using these three filters we decompose all the images separately and apply the soft-thresholding to the wavelet detail coefficients where the threshold is set to be 50% of the maximal detail coefficient intensity.

The final effect of the proposed method is presented in Fig. 4-a, while the effect of the conventional approach is presented in Fig. 4-b. In the resultant image (Fig. 4-a) the shadow (pixels with low intensity) is removed. This image has sharp edges of the vena and the heart, while the image in Fig. 4-b contains relatively high level of noise that blurs the edges of these objects. Therefore, the image in Fig. 4-a is more suitable for an upgrading expert system that could provide automatic identification of optimal shapes and positions of regions of interest needed for further physiological diagnostics.

The quality of the image in Fig. 4-b could be further improved by using certain low pass filtering techniques as shown in Fig. 4-c, but the projections of the vena and the heart would still suffer from certain deformations. These deformations could degrade the effects of an expert system for automatic identification of the optimal positions and shapes of regions of interest needed for further investigations.

VI. Conclusion

We present an approach on pre-processing heart region dynamic NM images. The images are processed in the DWT domain with linear phase NPR QMF filters. The filters are designed to have a cut-off frequency dependent on the images 2d-power spectrum. While filtering, particular image information from its adjacent images is used. The aim of this approach is to determine anatomical data in order to upgrade the software with an expert system that could identify the optimal positions and the shapes of the regions of interest needed for the heart study. We demonstrate the performance of the proposed method on real dynamic NM images, recorded and processed by our own upgraded gamma camera system developed at the department of NM in Bitola.

In view of the oval form of 2D Fourier transform of the images, the problem of processing NM images can be further extended by considering the possibility to apply wavelet shrinkage to the images by using different 1D filters for processing the images rows and columns, dependent on images 2D spectrum.

References

[1] General Electric, *Gamma Camera Technical Reference Manual*, 1980;

[2] Cvetko D. Mitrovski, “Quantitative Determination of Left-Right Shunt at Heart Disease Patients”, *Proceeding of papers,* Faculty of Technical Sciences – Bitola, pp. 327-335, 1996;

[3] G. Strang and T. Nguyen, *Wavelets and Filter Bank*s. Wellesley-Cambridge Press, 1996;

[4] D. L. Donoho, "Wavelet Thresholding and W.V.D.: A 10-minute Tour", *Int. Conf. on Wavelets and Applications*, Toulouse, France, June 1992;

[5] D. L. Donoho and I. M. Johnstone, "Ideal Spatial Adaptation via Wavelet Thresholding", *Biometrika*, vol. 81, pp. 425-455, 1994;

[6] Cvetko D. Mitrovski and Mitko B. Kostov, “On the Pre-processing of Dynamic Nuclear Medicine Images”, *International Scientific Conference on Information, Communication and Energy Systems and Technologies ICEST 2002*, Nis, Serbia and Montenegro, 2002;

[7] Cvetko D. Mitrovski and Mitko B. Kostov, “A Wavelet Approach on NM Images Filtering Using Adjacent Images Information”, *VII National Conference ETAI 2005*, Ohrid, Macedonia, Sept. 2005;

[8] Cvetko D. Mitrovski and Mitko B. Kostov, “On The Radionuclide Movement Depended Filtering Of Nuclear Medicine Images”, *Fourth International Conference for Informatics and Information Technology 2003*, Molika, Macedonia, Dec. 2003;

[9] Robert D. Nowak, Richard G. Baraniuk, ”Wavelet-Domain Filtering for Photon Imaging Systems”, *IEEE Trans. Image Processing*, vol. 8, Iss. 5, p. 666-678, May 1999;

[10] Xu, H., Lu, W.-S., and Antoniou, A. "A New Method for the Design of FIR Quadrature Mirror-Image Filter Banks," *IEEE Trans. Signal Processing*. vol. 45, pp. 1275-1281, July 1998.